



Mesoporous GaN Made by Selective Area Sublimation for Efficient Light Emission on Si Substrate

Benjamin Damilano, Stéphane Vézian, Jean Massies

► To cite this version:

Benjamin Damilano, Stéphane Vézian, Jean Massies. Mesoporous GaN Made by Selective Area Sublimation for Efficient Light Emission on Si Substrate. *physica status solidi (b)*, 2018, 255 (5), pp.1700392. 10.1002/pssb.201700392 . hal-03553871

HAL Id: hal-03553871

<https://hal.science/hal-03553871>

Submitted on 3 Feb 2022

HAL is a multi-disciplinary open access archive for the deposit and dissemination of scientific research documents, whether they are published or not. The documents may come from teaching and research institutions in France or abroad, or from public or private research centers.

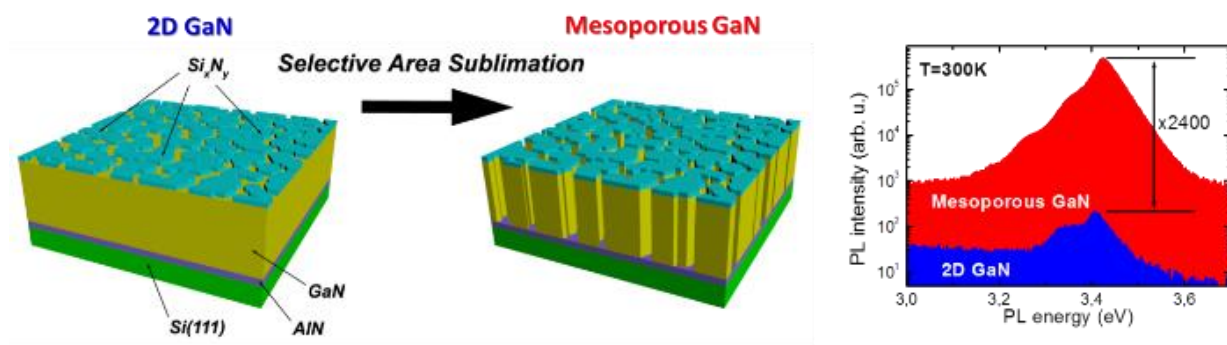
L'archive ouverte pluridisciplinaire **HAL**, est destinée au dépôt et à la diffusion de documents scientifiques de niveau recherche, publiés ou non, émanant des établissements d'enseignement et de recherche français ou étrangers, des laboratoires publics ou privés.

Mesoporous GaN made by selective area sublimation for efficient light emission on Si substrate.

B.Damilano,^{*} S. Vézian and J. Massies

Université Côte d'Azur, CNRS, CRHEA, France

Selective area sublimation of thin ($\leq 0.3 \mu\text{m}$) GaN-on-Si epitaxial layers through nanoholes of an incomplete monolayer of Si_3N_4 results in the formation of mesoporous GaN. This morphologic change from a 2-dimensional flat layer to a nanostructured material presents the unexpected property of a huge increase (> 3 orders of magnitude) of the GaN band edge photoluminescence intensity. Furthermore, the integrated photoluminescence intensity of such mesoporous GaN layers is comparable to a high quality $3.5 \mu\text{m}$ -thick GaN-on-sapphire epitaxial layer or a $350 \mu\text{m}$ -thick GaN substrate. Different possible mechanisms are discussed to explain the origin of the strong improvement of the optical properties.



^{*} Corresponding author: e-mail bd@crhea.cnrs.fr, Phone: +33 493 957 829, Fax: +33 493 958 361

1 Introduction

The revolution of solid-state lighting (SSL) is the keystone of the success story of GaN-on-sapphire epitaxial structures [1]. The next step will be to succeed in the development of GaN-on-Si epitaxial structures for both electronic and optoelectronic applications, because of the hegemonic role of Si in the electronic industry. This is close to achievement for GaN-based white light emitting diodes (LEDs) in the R&D laboratories of major companies involved in SSL [2,3]. But the performance/production cost ratio is presumably not yet sufficient to promote mass production and commercialization of GaN-on-Si LEDs. The main limiting factors are the complex architecture and the large thickness of the structures (4-5 μm) required to obtain high-quality LEDs on Si substrate. Moreover, the GaN material quality on Si remains too low to reach long lifetime laser devices, despite the recent demonstration of a CW blue laser diode [4]. This shows that a simple process for obtaining high quality GaN on Si still needs to be developed to fully exploit the possibilities of GaN-based device integration on Si. Some approaches are currently investigated to achieve this goal, such as, for example, GaN quantum dots [5], nanowires [6-8] or GaN growth on nanostructured Si substrates [9,10].

Here, we experiment a different approach. We show that transforming a very thin ($\leq 0.3 \mu\text{m}$) 2D GaN-on-Si layer into a mesoporous material, via a selective area sublimation (SAS) process [11], results in an increase by more than three orders of magnitude of the photoluminescence (PL) efficiency at room temperature. This opens a promising path for high quality and cost effective GaN-based devices on Si substrate.

2 Experimental

The samples are grown by molecular beam epitaxy (MBE) in a Riber reactor on Si(111) substrate using NH_3 as the N precursor and solid sources for Ga, Al, and Si elements. The growth temperature is measured by an Ircon infrared pyrometer ($\lambda=0.91\text{-}0.97 \mu\text{m}$), the emissivity is calibrated by using the silicon surface reconstruction transition $1\times 1 \leftrightarrow 7\times 7$ at 830°C . The substrates are de-oxidized chemically *ex situ* by a HF solution. For all the samples, the growth is initiated by 100 nm of AlN at 900°C . More details on the first stages of the growth of AlN on Si(111) can be found in Refs. [12,13]. The growth temperature is decreased to 780°C for the growth of a 70 or 250 nm-thick GaN layer. The ammonia flow rates are 50 cubic centimeter per minute for both AlN and GaN. The growth rates are 100 nm/h and 750 nm/h for AlN and GaN, respectively. The Si treatment of the GaN surface is performed at a temperature of 600°C . The Si cell temperature is set at 1220°C and the exposure time of the GaN surface varies from 5 to 75 min. The result of this process is the formation of a very thin (approximately 1 monolayer (ML) or less) Si_xN_y layer (or a SiGa_3N_3 ML as found by Markurt et al. [14]) giving rise to a $\sqrt{3}\times\sqrt{3}\text{R}30^\circ$ reconstruction observed by *in situ* reflection high-energy electron diffraction.

The samples with a GaN thickness of 70 nm or 250 nm are then annealed under vacuum at 900°C for 6 min. or 25 min., respectively, in order to selectively sublimate the GaN regions left uncovered by the Si_xN_y nanomask (Fig. 1) [11]. The first series of samples correspond to a GaN thickness of 70 nm and a variable Si exposure time: 5, 10, 15, 20, and 75 min. The second series of samples is based on a structure with 250 nm of GaN. The sample was cut in several pieces. One piece was kept as a reference. The other two pieces were re-introduced in the MBE chamber to be exposed to Si for 15 minutes or 75 minutes and annealed under

vacuum at 900°C for 25 min. Note that the time used for the GaN sublimation is significantly larger than the one used for the thinner GaN samples simply because more material has to be evaporated. A last sample is also grown with 250 nm of GaN and exposed to Si for 15 minutes. The rotation of the sample was stopped during the Si evaporation in order to force a gradient in the Si_xN_y coverage of the GaN surface. This sample is then annealed under vacuum at 900°C for 25 min. The presence of this gradient results in a variable porosity depending of the position on the sample.

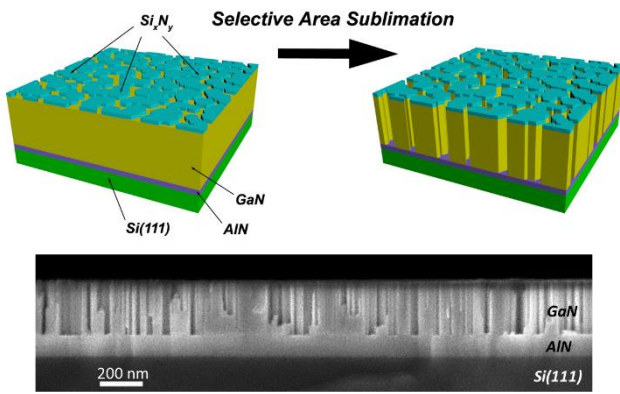


Figure 1 Fabrication of mesoporous GaN using selective area sublimation. The starting sample (left) is composed by a stack of GaN (70-250 nm) / AlN (100 nm) on a Si(111) substrate. The surface is exposed to Si to form an incomplete monolayer of Si_xN_y . The sample is then annealed at 900°C under vacuum to sublime the GaN regions left uncovered by the Si_xN_y nanomask (right). Cross-section scanning-electron microscopy image of mesoporous GaN-on-Si (bottom).

Photoluminescence experiments are performed at room temperature using the 244 nm line of a frequency doubled Ar-ion laser. The spot diameter is 130 μm . The excitation power density is 75 W/cm^2 . The light is collected by an optical fiber connected to an Acton SP558i spectrometer equipped by a grating with 150 lines/mm blazed at 500 nm. The signal is detected by a CCD Spec-10 100B cooled by liquid nitrogen.

A Supra 40 Carl Zeiss scanning electron microscope is used for the morphological characterization of the samples.

3 Results and discussion

Plane-view scanning electron microscopy (SEM) images on part of the first series of samples (70 nm of GaN on top of a 100 nm-thick AlN buffer layer) are shown in Fig. 2. For Si exposure times of 5-10 minutes (Fig. 2a and Fig. 2b), we observe the formation of small diameter (~ 10 nm) nanowires as found in our previous work [11]. For Si exposure times of 15-20 minutes (Fig. 2c), we do not observe anymore isolated nanowires but rather a nanoporous morphology. For the largest exposure time of 75 minutes, the surface is flat and only very few pits can be found as shown in Fig. 2d (note the larger scale compared to Fig. 2a-c). The Si_xN_y surface coverage is estimated from top-view SEM images corresponding to a total investigated area of 1 μm^2 . This

area is statistically representative of the surface morphology of the samples since the typical lateral size of the nanowires or nanopores is below 50 nm. The Si_xN_y surface coverage (Fig. 2e) varies from ~10% to 100% for a Si exposure time varying from 5 to 75 minutes. The pores extend vertically from the surface, almost down to the AlN layer, according to cross-section SEM images (see for example Fig. 1).

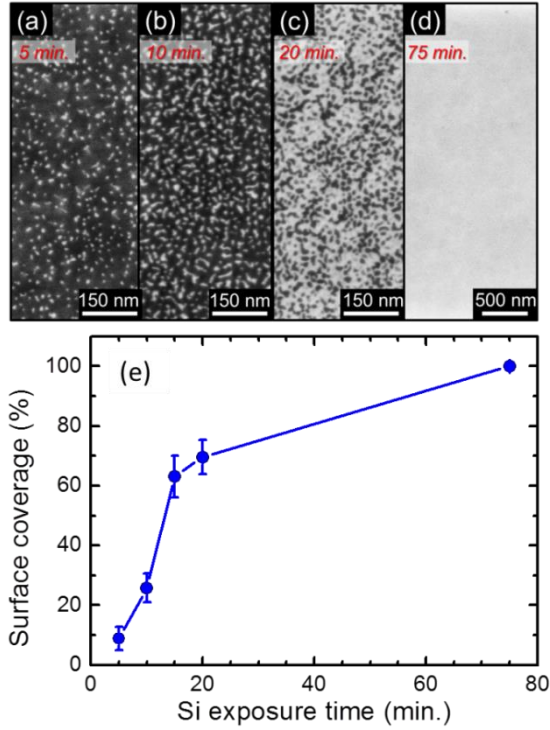


Figure 2 Scanning-electron microscopy images of samples constituted by GaN (70 nm) / AlN (100 nm) / Si(111) exposed to Si for various times : 5 (a), 10 (b), 20 (c), and 75 (d) minutes and annealed under vacuum during 6 minutes at 900°C. (e) Variation of the surface coverage of Si_xN_y after annealing as a function of the Si exposition time.

For PL experiments, we have chosen to study thicker GaN layers in order to have a complete absorption of the laser excitation in the GaN layer. At 244 nm (excitation laser wavelength), 90% of light is absorbed by 100 nm of GaN. Therefore, we grew the second series of samples (250 nm of GaN on a 100 nm-thick AlN buffer layer). For samples with similar structure (very thin GaN layer), a threading dislocation density of $2-3 \times 10^{10} \text{ cm}^{-2}$ was measured. As expected from the results shown above, the sample exposed to 75 minutes of Si kept a 2D flat morphology (Fig. 3a), while the sample exposed to 15 minutes of Si led to nanoporous GaN with an irregular pore shape (Fig. 3b). From Fig. 3b we estimate that the minimum pore size is a few nm and the maximum can reach 50 nm, which is at least 3-5 times smaller than in the works of Bilousov et al. [15], Pandey et al. [16] or Yu et al [17].

Fig. 3c shows the room temperature PL spectra of the three samples: the 2D-GaN, the annealed 2D-GaN (covered by a complete Si_xN_y mask before annealing), and the mesoporous GaN. All the spectra are

dominated by a PL peak around 3.4 eV which is characteristic of the GaN band-edge emission. The full-width-at-half-maximum of this peak is 49 meV, 45 meV, and 48 meV for the 2D-GaN sample, the annealed 2D-GaN sample, and the mesoporous GaN sample, respectively. The spectrum of the 2D-GaN sample shows a shoulder at about 3.34 eV attributed to the first LO phonon replica of the main peak with a Huang-Rhys factor of ~ 0.5 . This shoulder is also present on the other two samples but the Huang-Rhys factor decreases down to ~ 0.2 . Both the 2D-GaN and annealed 2D-GaN samples have approximately the same PL intensity, while the PL signal of the mesoporous sample is 2400 times more intense. More accurately, the integrated PL intensity ratio between the mesoporous GaN and the 2D-GaN sample is 1700. This increase of the PL intensity first shows that the non-radiative surface recombination velocity at the pore edges is small, meaning that the pore sidewalls are not damaged by the thermal treatment. The origin of this strong PL intensity enhancement can be related to several factors: an improvement of the structural quality (decrease of the density of point defects or extended defects such as dislocations), a stronger light extraction efficiency, and a higher doping level. As the GaN is annealed at higher temperature than the growth temperature, it is possible that point defects are cured during this process. However, no improvement of the PL intensity is observed for the annealed 2D GaN layer. Therefore we can discard this hypothesis.

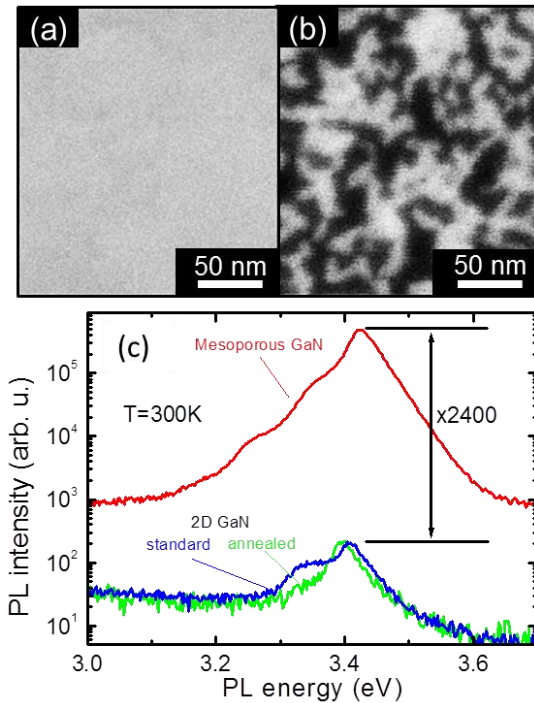


Figure 3 (a) Scanning-electron microscopy images of a sample constituted by GaN (250 nm) / AlN (100 nm)/ Si(111) exposed to Si for 75 minutes and annealed under vacuum for 25 minutes. (b) Same sample structure but with an exposition to Si for only 15 minutes. (c) Comparison of the room temperature photoluminescence spectra of these two samples and the standard sample GaN (250 nm) / AlN (100 nm)

without Si exposure and annealing. The peak photoluminescence intensity of the mesoporous GaN sample is 2400 times larger than the two other samples (standard and annealed).

When the roughness of the GaN layer increases, the light extraction can also increase, as it has been reported for GaN-based LEDs with a nanotextured top surface in Ref. [18]. Unlike the works corresponding to Refs. [15-18], the characteristic size d of the pores of the nanoporous GaN sample is below 50 nm, i.e. largely subwavelength (the GaN peak emission wavelength is $\lambda=365$ nm) and therefore the Mie scattering by such nanostructures is very weak as it varies as $(d/\lambda)^4$ in the Rayleigh approximation. Actually, the most important effect is expected to be a decrease of the refractive index of the layer with such a non-periodic subwavelength porosity [19]. The refractive index variation as a function of the porosity has been exploited for the fabrication of high-reflectivity and low-strained GaN-based distributed Bragg reflector or for light confinement in edge-emitting laser diodes [20,21]. In the effective medium approximation, the average dielectric function leads to an index change given by [20]:

$$n_{eff} = \sqrt{(1-p)n^2 + p} \quad (1)$$

where n is the refractive index of GaN, and p its porosity.

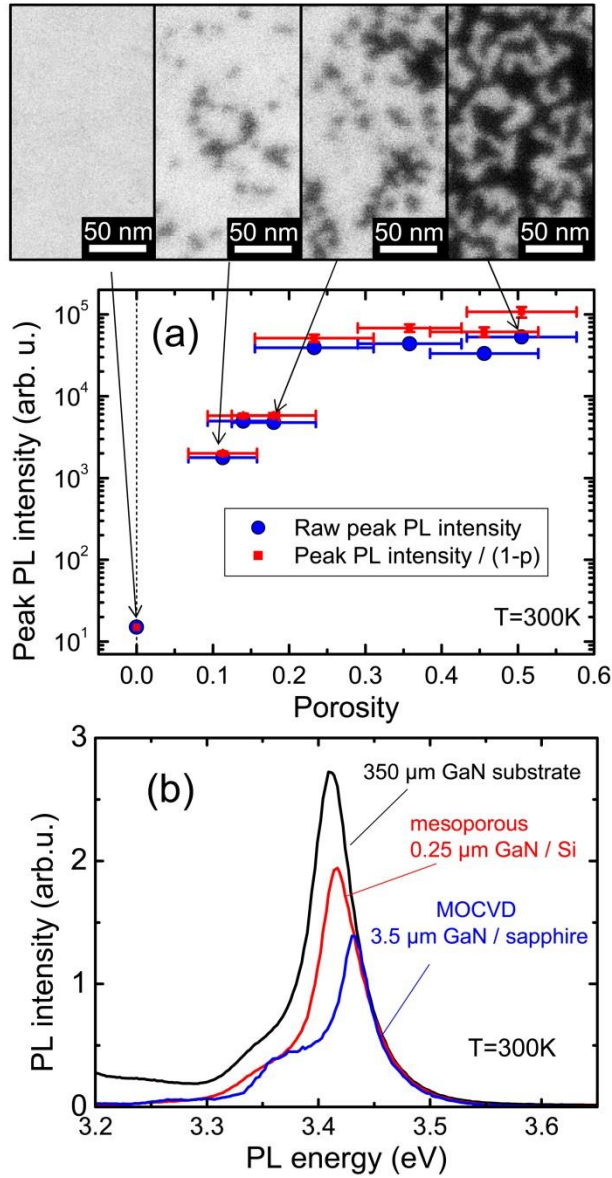


Figure 4 (a) Variation of the room-temperature photoluminescence intensity as a function of the GaN porosity for samples constituted by GaN (250 nm) / AlN (100 nm) / Si(111). (b) Comparison of the room-temperature photoluminescence intensity of a mesoporous GaN (250 nm) / AlN (100 nm) / Si(111) and commercially available GaN samples: a 3.5 μm -thick GaN layer grown on sapphire by metal-organic chemical vapor deposition (from Saint-Gobain-Lumilog) with a dislocation density of $\sim 4 \times 10^8 \text{ cm}^{-2}$, and a 350 μm -thick GaN substrate (from Ammono) with a dislocation density $< 5 \times 10^4 \text{ cm}^{-2}$.

The light extraction efficiency for one side can be roughly estimated by $1/4n^2$ [22]. Applying these formula for a porosity of 0.5 (corresponding to the case of sample of Fig. 3b), we find an increase of the light

extraction of 80%. Therefore, this effect cannot be the main reason for the three orders of magnitude increase of the PL intensity.

Also, it is well known that GaN n-type doping with Si can affect the room temperature PL yield [23]. Heavy Si doping (donor concentration of $7 \times 10^{18} \text{ cm}^{-3}$) can enhance the PL intensity of doped samples by a factor 10 compared to undoped GaN layers [23]. As the samples considered here are covered by a Si-based compound and annealed at high temperature, Si diffusion in GaN can be suspected. Indeed, the decrease of the Huang-Rhys factor indicates a larger density of donors in the annealed samples [24]. However, the linewidth of the GaN band-edge peak does not increase significantly compared to the reference sample. A strong increase of the Si doping would result in a significant broadening of the GaN PL peak [23,24]. The PL intensities of the 2D annealed sample and the reference sample are comparable. These observations show that the doping increase is rather limited and cannot be the main origin for the PL intensity enhancement for the mesoporous sample.

One of the main hypotheses remains: an improvement of the material quality due to a decrease of the dislocation density. Indeed, it has been shown that etching of GaN layers at high temperature in a metal-organic chemical vapor deposition (MOCVD) reactor leads to a preferential decomposition of GaN at the dislocation location [25].

Fig. 4a shows the variation of the room temperature PL intensity as a function of the GaN porosity (defined as $1-\theta$, where θ is the fraction of Si_xN_y covered GaN surface). Starting from a 2D GaN layer (porosity=0), we see a very rapid increase of the PL intensity. For porosity of 0.11, the PL intensity increases by 2 orders of magnitude. For porosity of 0.25-0.5, the PL intensity is more than three orders of magnitude larger than the reference 2D GaN layer. Note that for porous layers, the surface excited by the laser is decreased by factor $1-p$ due to the removal of GaN material. Therefore, in Fig. 4a the PL intensity should be increased by a factor $1/(1-p)$ to take into account the fact that porous layers absorb less light than non-porous layers. Finally, we compared the room temperature PL spectra of a $0.25 \text{ }\mu\text{m}$ -thick mesoporous GaN sample (porosity of 0.5) with a high-quality commercially available (Saint-Gobain-Lumilog) [26] $3.5 \text{ }\mu\text{m}$ -thick GaN layer grown on a sapphire substrate by MOCVD and a $350 \text{ }\mu\text{m}$ -thick GaN substrate from Ammono (Fig. 4b) [27]. The threading dislocation density measured on the Lumilog sample is $\sim 4 \times 10^8 \text{ cm}^{-2}$, a typical dislocation density for the fabrication of high efficiency blue and white LEDs. The threading dislocation density of the Ammono GaN substrate is $< 5 \times 10^4 \text{ cm}^{-2}$ which is the state of the art of the GaN structural quality. The integrated PL intensity of the mesoporous GaN-on-Si layer is 1.4 times higher than the one of the MOCVD GaN-on-sapphire sample and 1.4 times smaller than the one of the GaN substrate. This illustrates the luminescence efficiency achieved with a thin GaN mesoporous layer. For thermodynamics reasons, preferential evaporation of GaN should occur where crystal defects (such as dislocations) emerge at the free surface, i.e. uncovered by the Si_xN_y mask. Of course, dislocations present in the unprotected GaN areas have disappeared with the GaN sublimation, but there is no obvious reason why the major part of the dislocations present in the 2D layer should be concentrated in the uncovered material: statistically, roughly the same density of dislocations should be present in the covered and uncovered regions. Therefore, other mechanisms should be at work in the mesoporous GaN to explain the huge increase of the luminescence efficiency. Among these, it can be suggested that a significant part of the dislocations located below the Si_xN_y protective layer migrates towards the free-edge $\{1-100\}$ surfaces induced by the nanopore formation during the annealing procedure and,

therefore, the threading dislocation density decreases. Such a mechanism can well explain why nanowires obtained by SAS and studied in Ref. [11] are free from dislocations. It is also possible that the Si_xN_y could preferentially form on dislocation-free regions. A last explanation is that the pores act as local lateral confinement barriers which inhibit the diffusion of exciton towards dislocations, similarly to the case of quantum dots. However, complementary investigations will be necessary to completely understand the results and validate or refute the interpretations suggested here.

4 Conclusion

In summary, it is shown that selective area sublimation applied to thin GaN-on-Si epitaxial layers using an appropriate Si_xN_y protective mask gives rise to mesoporous GaN. The room-temperature (RT) photoluminescence intensity starts to strongly increase even for a low porosity of 0.1 and for a porosity of 0.4 an increase of more than 3 orders of magnitude of the photoluminescence intensity is observed by comparison with the GaN-on-Si layer before SAS. The RT integrated photoluminescence intensity of such mesoporous GaN is even higher than the one obtained on a $3.5\ \mu\text{m}$ low dislocation density ($4 \times 10^8\ \text{cm}^{-2}$) GaN-on-Sapphire high-quality epitaxial layer grown by MOCVD. Several mechanisms which can be invoked to explain such results are briefly discussed. From this preliminary discussion and within our present knowledge, it appears that only the reduction of the dislocation density can explain the huge increase of the PL efficiency observed. Other complementary investigations, such as transmission electron microscopy, will be however necessary to complete the analysis of the obtained results. Nevertheless, the approach used here for simple thin GaN-on-Si layers can be probably transposed for device structures using a vertical transport of the electrical carriers and requiring a high material quality on Si substrate.

Acknowledgements The authors would like to thank J. Brault for continuous help and interest, E. Frayssinet and D. Lefebvre for their skilled technical assistance, J.M. Chauveau, Y. Cordier, P. Genevet, and M. Leroux for helpful discussions and J. Y. Duboz, F. Semond for the critical reading of the manuscript.

References

- [1] S. Nakamura, Rev. Mod. Phys. **87**, 1139 (2015).
- [2] B. Hahn, B. Galler, and K. Engl, Jpn. J. Appl. Phys. **53**, 100208 (2014).
- [3] L. Zhang, W.-S. Tan, S. Westwater, A. Pujol, A. Pinos, S. Mezouari, K. Stribley, J. Whiteman, J. Shannon and K. Strickland, IEEE J. Electron Devices Soc. **3**, 457 (2015).
- [4] Y. Sun, K. Zhou, Q. Sun, J. Liu, M. Feng, Z. Li, Y. Zhou, L. Zhang, D. Li, S. Zhang, M. Ikeda, S. Liu and H. Yang, Nat. Photonics **10**, 595 (2016).
- [5] B. Damilano, J. Brault, and J. Massies, J. Appl. Phys. **118**, 024304 (2015).
- [6] R. Yan, D. Gargas, and P. Yang, Nat. Photonics **3**, 569 (2009).

- [7] H. P. T. Nguyen, S. Zhang, A. T. Connie, M. G. Kibria, Q. Wang, I. Shih and Z. Mi, *Nano Lett.* **13**, 5437 (2013).
- [8] K. Kishino and S. Ishizawa, *Nanotechnology* **26**, 225602 (2015).
- [9] C. B. Han, C. He and X. Li, *J. Adv. Mater.* **23**, 4811 (2011).
- [10] D. R. Kim, C. H. Lee, I. S. Cho, H. Jang, M. S. Jeon and X. Zheng, *ACS Nano*, DOI 10.1021/acsnano.7b01967 (2017).
- [11] B. Damilano, S. Vézian, J. Brault, B. Alloing and Massies, *Nano Lett.* **16**, 1863 (2016).
- [12] F. Semond, Y. Cordier, N. Grandjean, F. Natali, B. Damilano, S. Vézian and J. Massies, *Phys. Status Solidi A* **188**, 501 (2001).
- [13] A. Le Louarn, S. Vézian, F. Semond and J. Massies, *J. Cryst. Growth* **311**, 3278 (2009).
- [14] T. Markurt, L. Lymperakis, J. Neugebauer, P. Drechsel, P. Stauss, T. Schulz, T. Remmele, V. Grillo, E. Rotunno and M. Albrecht, *Phys. Rev. Lett.* **110**, 036103 (2013).
- [15] O. V. Bilousov, J. J. Carvajal, H. Geaney, V. Z. Zubialeovich, P. J. Parbrook, O. Martínez, J. Jiménez, F. Díaz, M. Aguiló and C. O'Dwyer, *ACS Appl. Mater. Interfaces* **6**, 17954 (2014).
- [16] P. Pandey, M. Sui, M.-Y. Li, Q. Zhang, S. Kunwar, J. Wu, Z. M. Wang, G. J. Salamo and J. Lee, *Cryst. Growth & Des.* **16**, 3334 (2016).
- [17] J. Yu, L. Zhang, J. Shen, Z. Xiu and S. Liu, *CrystEngComm* **18**, 5149 (2016).
- [18] S. Chhajed, W. Lee, J. Cho, E. F. Schubert and J. K. Kim, *Appl. Phys. Lett.* **98**, 071102 (2011).
- [19] M. M. Braun and L. Pilon, *Thin Solid Films* **496**, 505 (2006).
- [20] C. Zhang, S. H. Park, D. Chen, D.-W. Lin, W. Xiong, H.-C. Kuo, C.-F. Lin, H. Cao, J. Han, *ACS Photonics* **2**, 980 (2015).
- [21] G. Yuan, K. Xiong, C. Zhang, Y. Li and J. Han, *ACS Photonics* **3**, 1604 (2016).
- [22] E. F. Schubert, *Light-emitting diodes*, 2nd ed. (Cambridge University Press, Cambridge, New York, 2006).
- [23] E. F. Schubert, I. D. Goepfert, W. Grieshaber, J. M. Redwing, *Appl. Phys. Lett.* **71**, 921 (1997).
- [24] M. Leroux, B. Beaumont, N. Grandjean, P. Lorenzini, S. Haffouz, P. Vennéguès, J. Massies and P. Gibart, *Mater. Sci. Eng. B* **50**, 97 (1997).
- [25] Y. Tian, L. Zhang, Y. Wu, Y. Shao, Y. Dai, H. Zhang, R. Wei and X. Hao, *CrystEngComm* **16**, 2317 (2014).
- [26] <http://www.ceramicmaterials.saint-gobain.com/lumilog>

[27] <http://www.ammono.com/>